Electronic Supplementary Material (ESI) for Energy & Environmental Science.

Supporting Information

Shear-flow induced alignment of graphene enable the closest packing crystallography of (002) textured zinc metal anode with high-reversibility

Murong Xi [1a], Zhenjie Liu [1a], Wei Wang [a], Zihan Qi [a], Rui Sheng [a], Juan Ding [a]. Yudai Huang [a, *], Zaiping Guo [b, *]

[a] State Key Laboratory of Chemistry and Utilization of Carbon Based Energy Resources, College of Chemistry, Xinjiang University, Urumqi 830017, Xinjiang, China

[b] School of Chemical Engineering, Faculty of Sciences, Engineering and Technology, The University of Adelaide, SA 5005, Australia

Email address: huangyd@xju.edu.cn; zaiping.guo@adelaide.edu.au

Keywords: Shear-flow induced, Graphene-modified copper current collector, Dendritic-free, High-reversible, Zinc anode

Experimental Section:

Preparation of graphene ink: graphene (CPG1808, http://jutan.net.cn/) is dispersed into ethanol, where the concentration of graphene is controlled at 15wt%-20wt%. In addition, 5% wt of poly(vinyl butyral) (PVB, Aladdin, M.W. 40,000-70,000) (graphene-based mass) is added as an auxiliary dispersant and binder.

Preparation of graphene-modified copper collector: The above graphene ink was coated on the surface of Cu foil by means of knife coating method, in which the thickness of the scraped liquid film should be lower than the sheet diameter of graphene. The average size of graphene selected in this work is 5-10 μm, so we chose the thickness of scratch coating as 5 μm in this experiment.

Preparation of Cu@G@Zn, Cu@Zn anodes: Fixed capacity Zn deposition was carried out at a current density of 40 mA cm^{-2} in a two-electrode system (Cu@G and Cu as the working electrode, and Zn as the counter electrode and reference electrode). In this work, the electrolyte is 2M $ZnSO_4$ ($ZnSO_4 \cdot 7H_2O$, > 99.995%, Aladdin). For the Zn-MnO_2 double-plated cell, the electrolyte is 2M $ZnSO_4$ and 0.1M H_2SO_4+0.4 $MnSO_4$ (99.995%, Aladdin).

Preparation of AC, PANI cathodes: The AC cathode was prepared by mixing AC-YP50F powder, carbon nanotubes (CNTs) and PVDF with a weight ratio of 8:1:1 in 1-methyl-2-pyrrolidone. The PANI cathode was prepared by mixing PANI, AC and PVDF with a weight ratio of 7:2:1 in 1-methyl-2-pyrrolidone solution. Then, the slurry solutions were cast onto carbon papers by the doctor blading method and dried at 80 °C for 12 h under vacuum. After drying, the electrodes were cut into discs with diameters of 12 mm, and the mass loading of AC and PANI is approximately 1-1.5 mg.

Cell assembly: The Zn foils (thickness = 100μm) was used without further treatment. All electrodes were cut into Φ12 mm discs. Glass fiber separator (GF/A, from Olegeeino, cut into Φ16 mm) was used as the separator and 2M $ZnSO_4$ was used as the electrolyte. For Zn//Cu and Zn//Cu@G cells, pristine Zn and Cu or Cu@G was assembled into the 2032 coin-type cells with 80 μL electrolyte.

Characterization: The phases of Cu@G@Zn, Cu@Zn were characterized by X-ray

diffraction (XRD, Bruker D8 Advance equipped with Cu Kα radiation, Germany) and the morphology was characterized by field-emission scanning electron microscopy (SEM, Hitachi FE-SEM S-4800, Japan).

Electrochemical Measurements: Cyclic voltammetry (CV) and linear sweep voltammetry (LSV) curves were obtained by an electrochemical workstation (CHI 760E). The galvanostatic charge/discharge (GCD) measurements were performed by a battery test system (CT2001A, LAND) and NEWARE Battery Test System (MHW-300-5V12A80CH-380V-3C, Shen-zhen,China). The electrochemical impedance spectra (EIS) were measured in a frequency range from 10 mHz to 1 MHz with an AC voltage amplitude of 5 mV (ZAHNER-elektrik electrochemical workstation).

Computational Methods: The density functional theory (DFT) calculations have been conducted on Vienna ab-initio simulation package (VASP) [1] to study the adsorption process on prepared materials. The Projector augmented wave method [1b] with a cutoff energy of 400 eV accompanied by Perdew-Burke-Ernzerhof functional [2] has been used in the DFT calculations. DFT-D3 method [3] was used to correct the van der Waals interactions, respectively. The (002), (101) and (100) facets of Zn crystal have been cleaved with a vacuum layer of 15 Å to build the slab models, respectively. All models have been fully relaxed with the energy convergence criterion of 10^{-6} eV and the force convergence criterion of 0.02 eV/Å, respectively. The Brillouin zone integration was performed with the Γ-point. The adsorption energy (E_{ads}) has been calculated using formula 1,

$$E_{ads} = E_{total} - E_{substrate} - E_{adsorbate} \quad (1)$$

The E_{total}, $E_{substrate}$ and $E_{adsorbate}$ represent the energy of adsorption structure, substrate and adsorbate, respectively. The free energies have been calculated using the following formula 2,

$$G = E_{DFT} + ZPE - TS \quad (2)$$

The G, E_{DFT}, ZPE and TS represent the free energy, energy from DFT calculations, zero point energy and entropic contributions, respectively. The authors extend their gratitude to Theoretical and Computational Chemistry Team from Shiyanjia Lab (www.shiyanjia.com) for providing invaluable assistance.

The ion transport for the Zn anode was predicted with a 2D Nernst-Planck formulation accounting for diffusion and migration in the bulk electrolyte and separators. The modeling domain, geometrical dimensions, and major boundary conditions are shown in Figure 5a, b in the manuscript. The governing equations for Zn anode with polyacrylonitrile membrane were given as formula 3 and 4.

$$\nabla^2\varphi = -F\sum z_i C_i \quad (3)$$

$$\frac{\partial C_i}{\partial t} = \nabla\cdot\left[D_i\nabla C_i + \frac{D_i C_i}{RT} z_i \nabla\varphi\right] \quad (4)$$

where *F*, *R* and *T* are the Faraday constant, ideal gas constant and temperature, D_i is the diffusion coefficient (1×10^{-10} m^2 s^{-1} for Zn^{2+} and 1.38×10^{-9} m^2 s^{-1} for SO_4^{2-}), C_i is the concertation, z_i is the charge number, and φ is the electrolyte potential. Electroneutrality was assumed throughout the whole domains. In the experiment, the flux of Zn^{2+} is uniform through uniform pore structure and ion conductive polyacrylonitrile membrane. The experimental current is 3 mA cm^{-2}, the electrode length is 5 microns, and the overall diffusion distance of electrolyte is 2 microns. A model with bubbles and initial structure is established to obtain the concentration distribution and electric field distribution in different deposition states (Figure 5a, b). The processed electrochemistry model was imported into the finite element software COMSOL® (Stockholm, Sweden), where the material properties were defined and the relevant problems were calculated and analyzed. To solve the discretized transport and electrode deformation kinematics equations, the Parallel Direct Sparse Solver (PARDISO) was employed. Time stepping was handled using the 2nd order backward Euler differentiation.

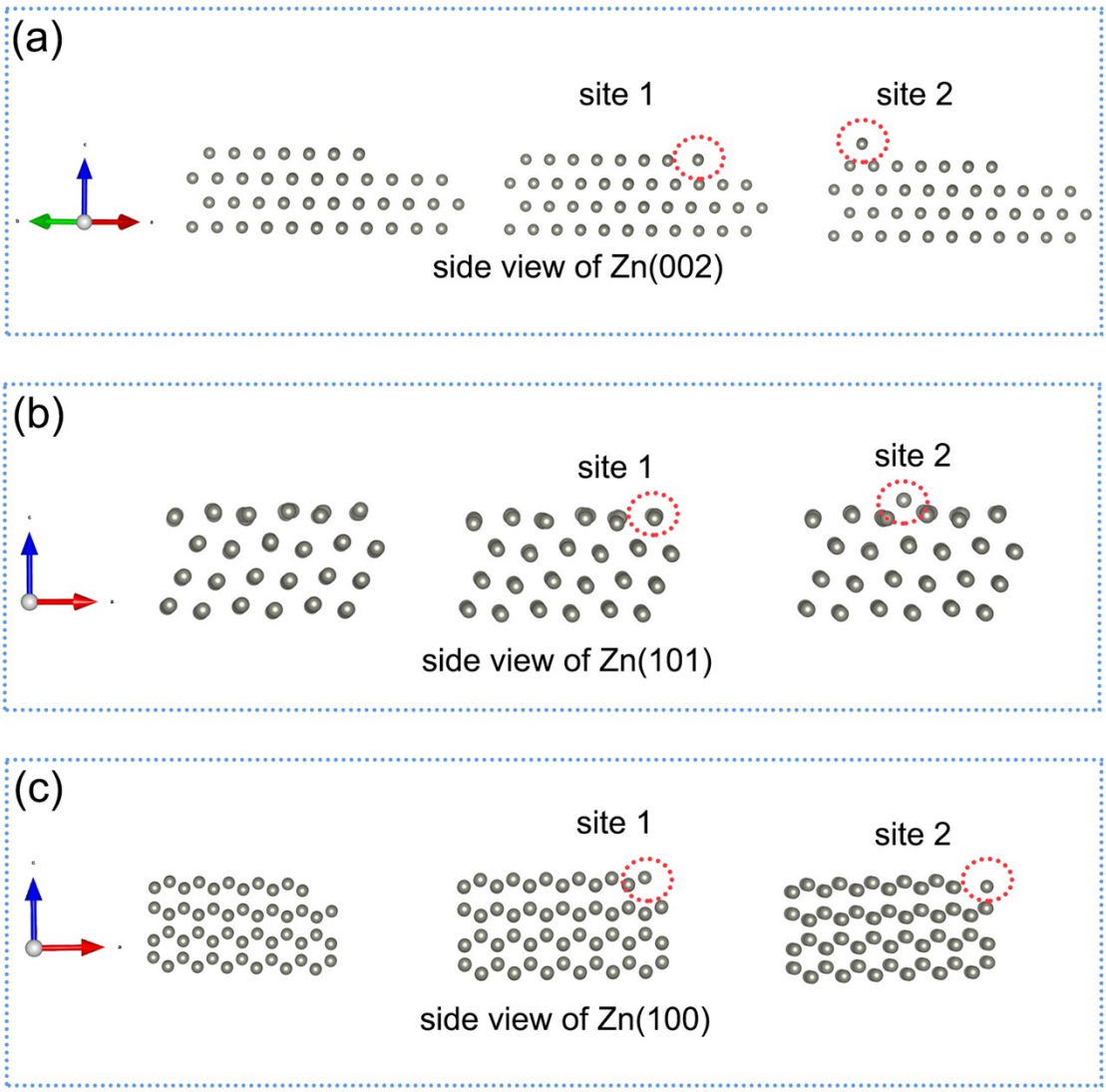

Figure S1. (a-c) Initial and side view of the calculation models of Zn absorbed on the (a) Zn (002), (b) Zn (101), and (c) Zn (100).

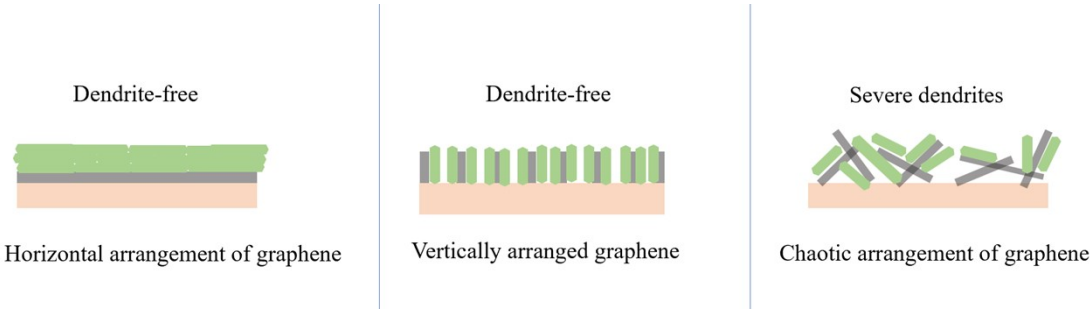

Figure S2. Diagram of Zn plating on different forms of graphene.

Figure S3. Contact angle of graphene ink on Cu foil surface.

Figure S4. Optical photograph about experimenter demonstrating prepared large-area Cu@G collector.

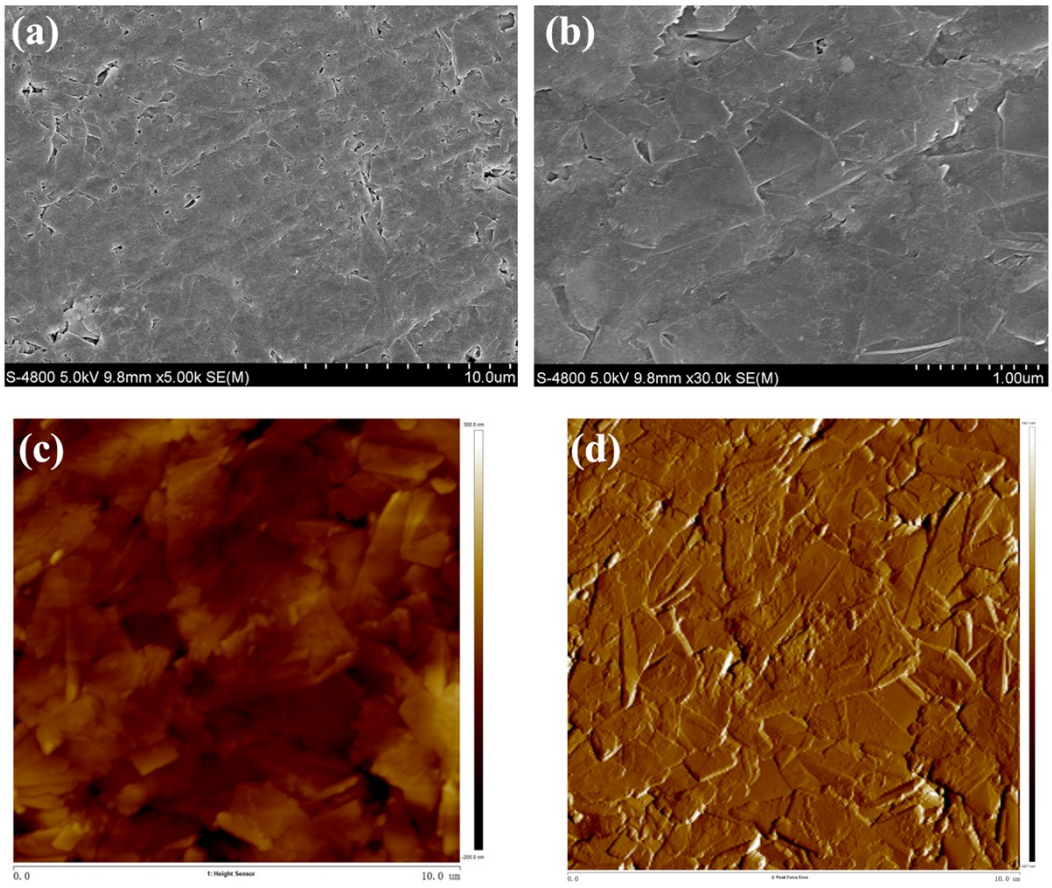

Figure S5. (a,b) SEM images and (c,d) AFM images of the prepared Cu@G collector .

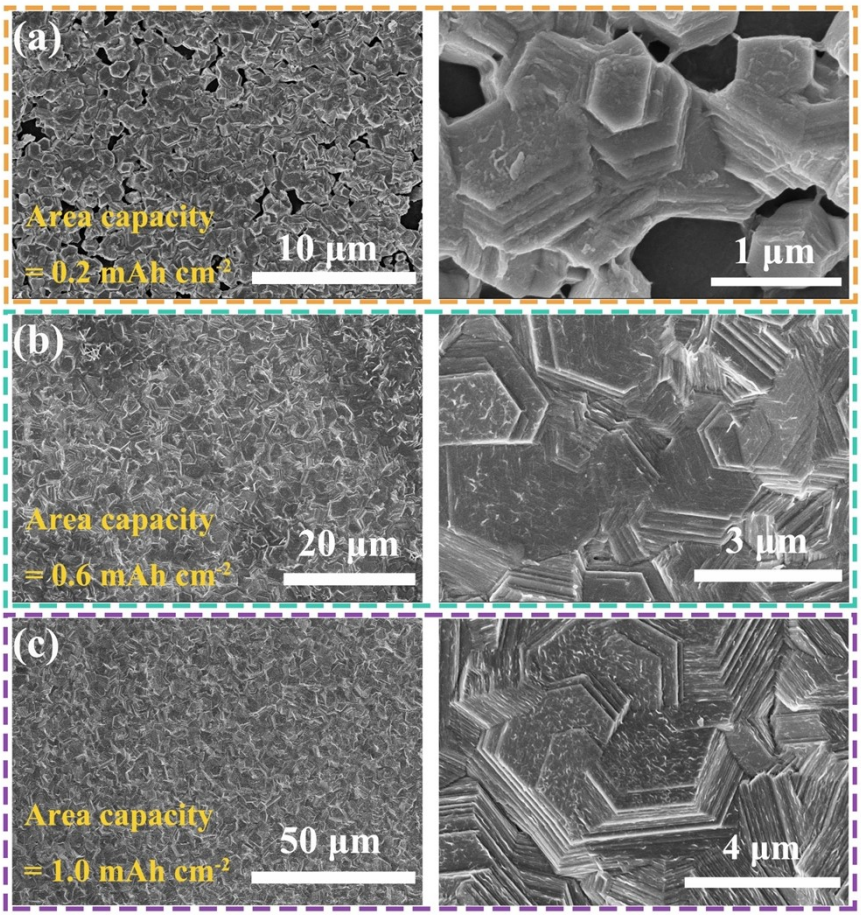

Figure S6. SEM images of Zn plated on Cu@G at 40 mA cm^{-2} with different area capacity.

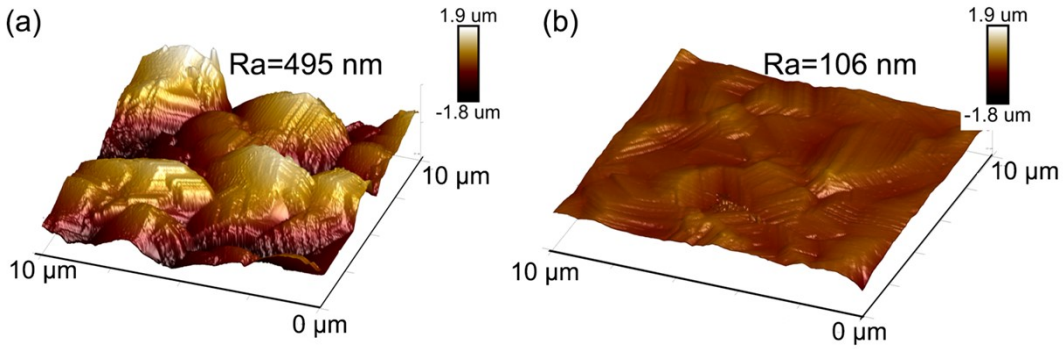

Figure S7. AFM images of Zn plated on (a) Cu and (b) Cu@G at 40 mA cm^{-2} with 1.5 mA h cm^{-2}.

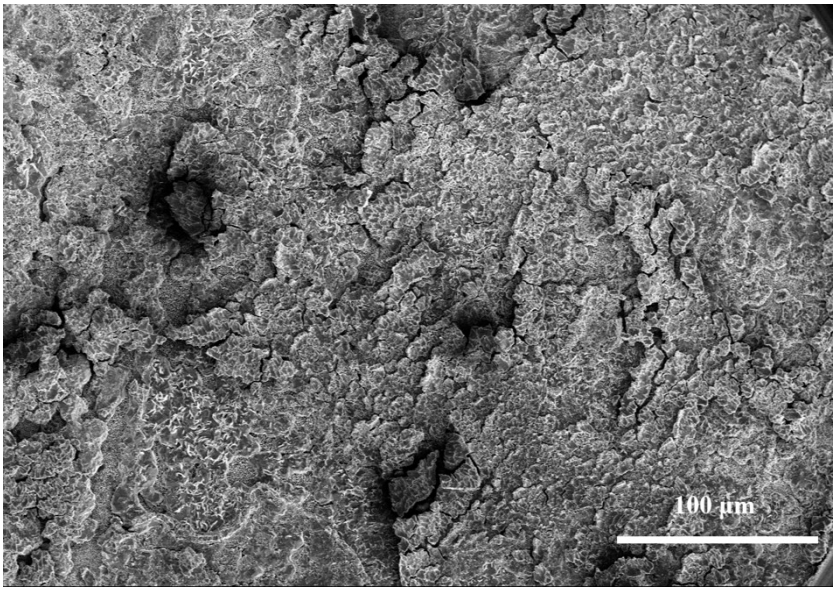

Figure S8. SEM image of Zn plated on Cu at 40 mA cm^{-2} with 1.5 mA h cm^{-2}.

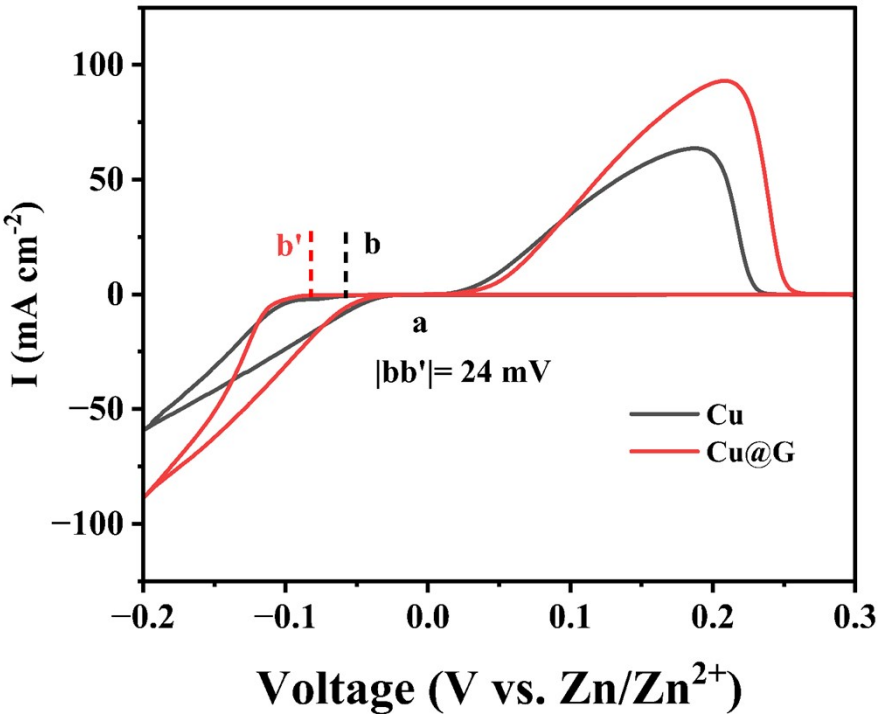

Figure S9. CV curves of Zn on Cu and Cu@G collectors.

A crossover characteristic can be observed as the positive sweeping potentials and the crossover potential is located at the point (a). The potential difference between the crossover point (a) and the point (b or b') is considered as the nucleation overpotential. In this work, the current density=0 line is used as the reference line to calculate the points b and b'.

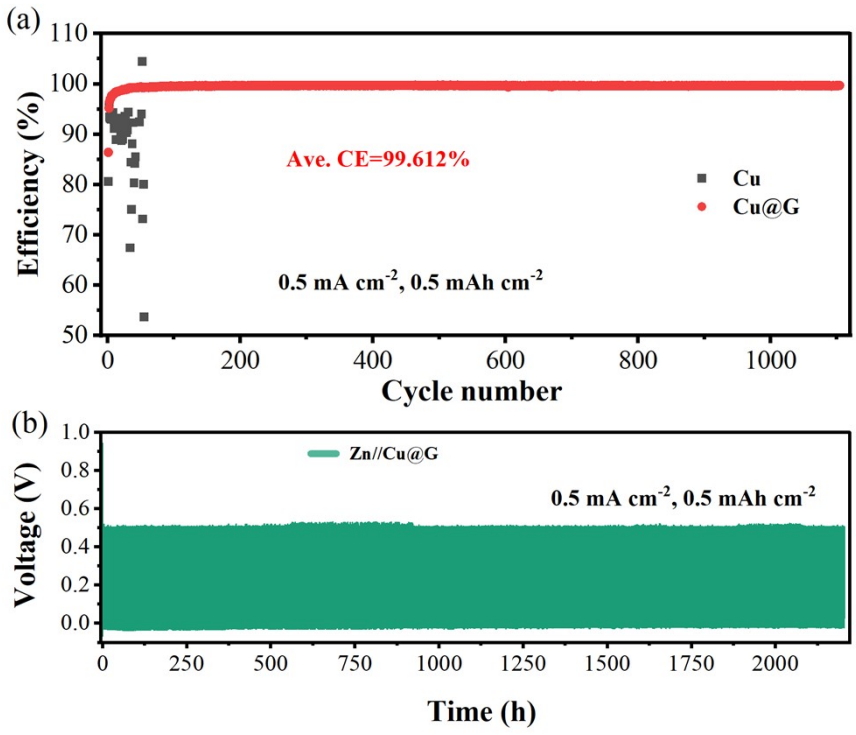

Figure S10. (a) ACE of Cu and Cu@G at 0.5 mA cm^{-2} with 0.5 mA h cm^{-2} and (b) corresponding voltage-time curve of Zn//Cu@G half battery.

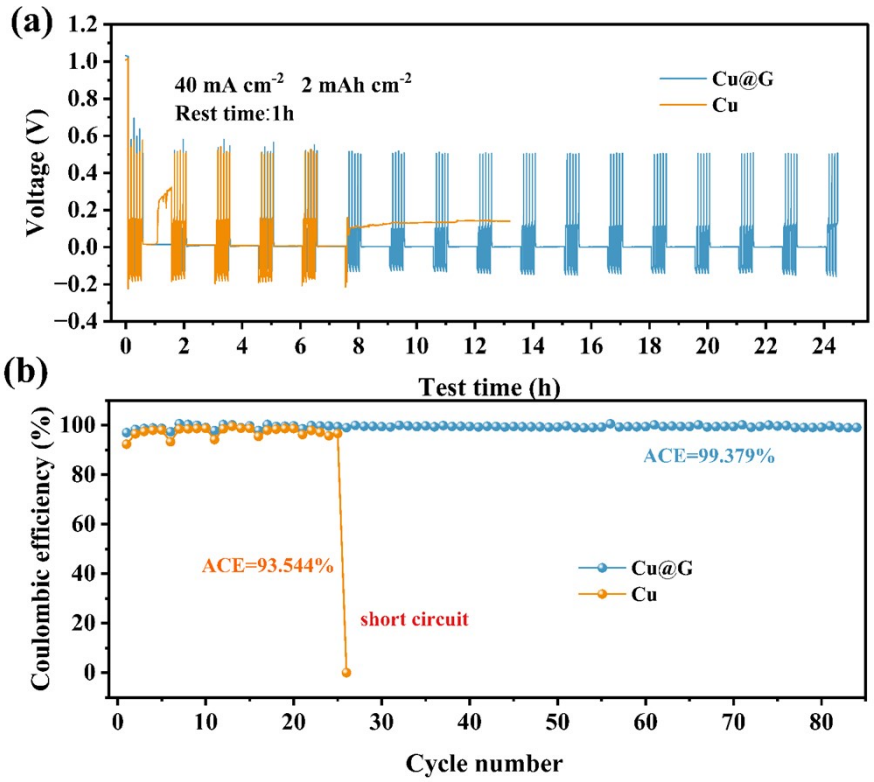

Figure S11. (a) Shelving-recovery performance, and (b) the ACE of Cu and Cu@G collector.

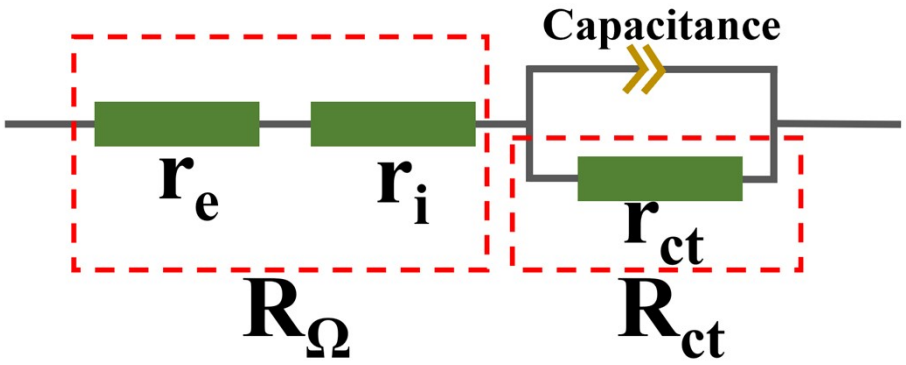

Figure S12. Equivalent circuit diagram for normal condition.

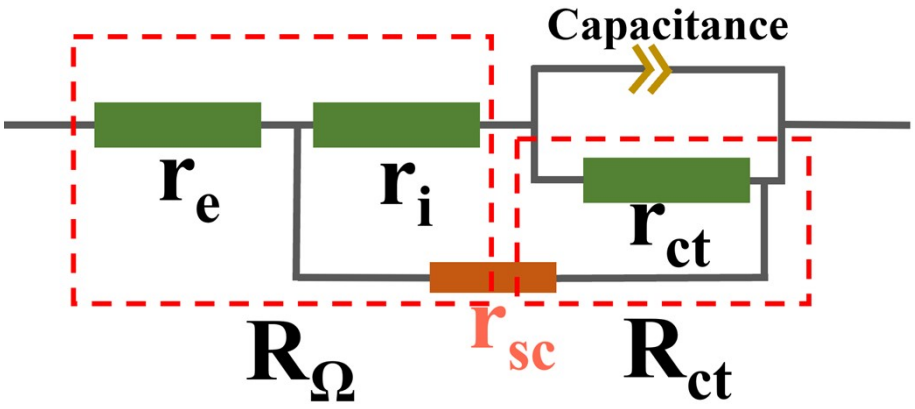

Figure S13. Equivalent circuit diagram for soft shorts.

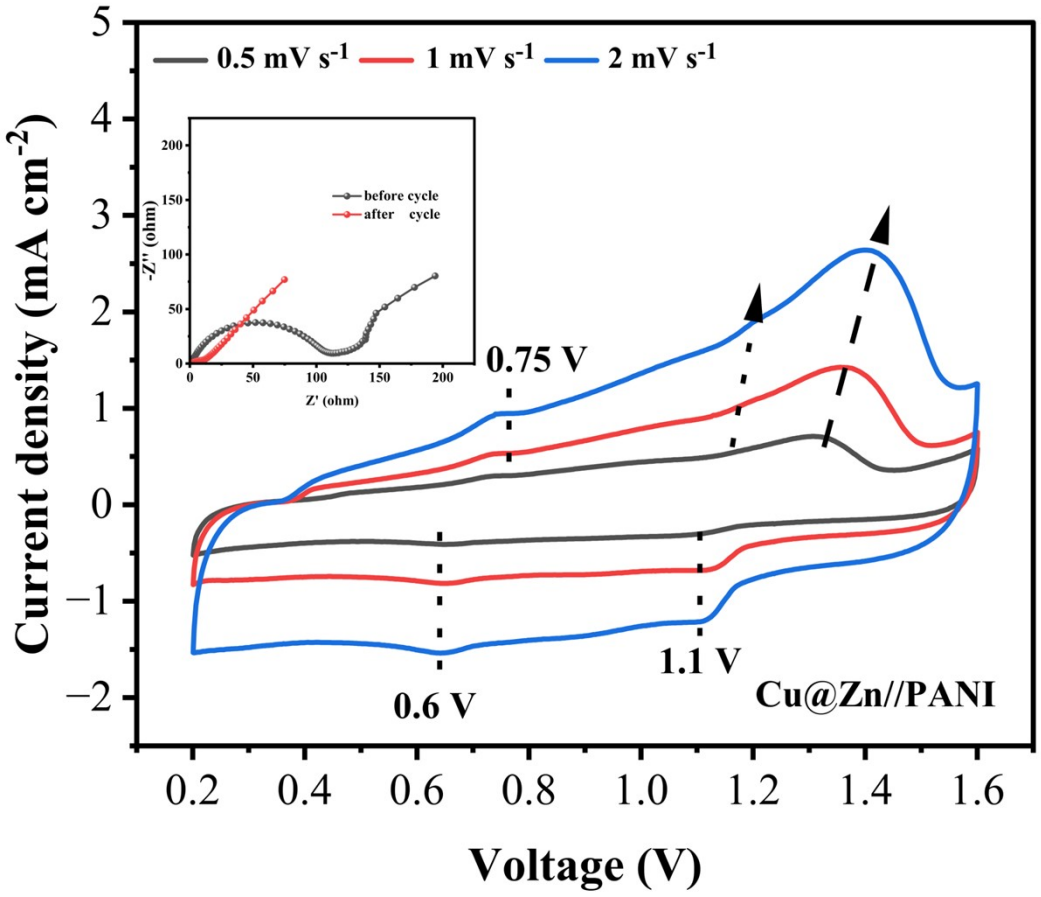

Figure S14. CV curves of Cu@Zn//PANI battery at different scan rate with N/P=4.5, inset: EIS spectra of Cu@G@Zn//PANI battery before and after cycle at different scanning rates

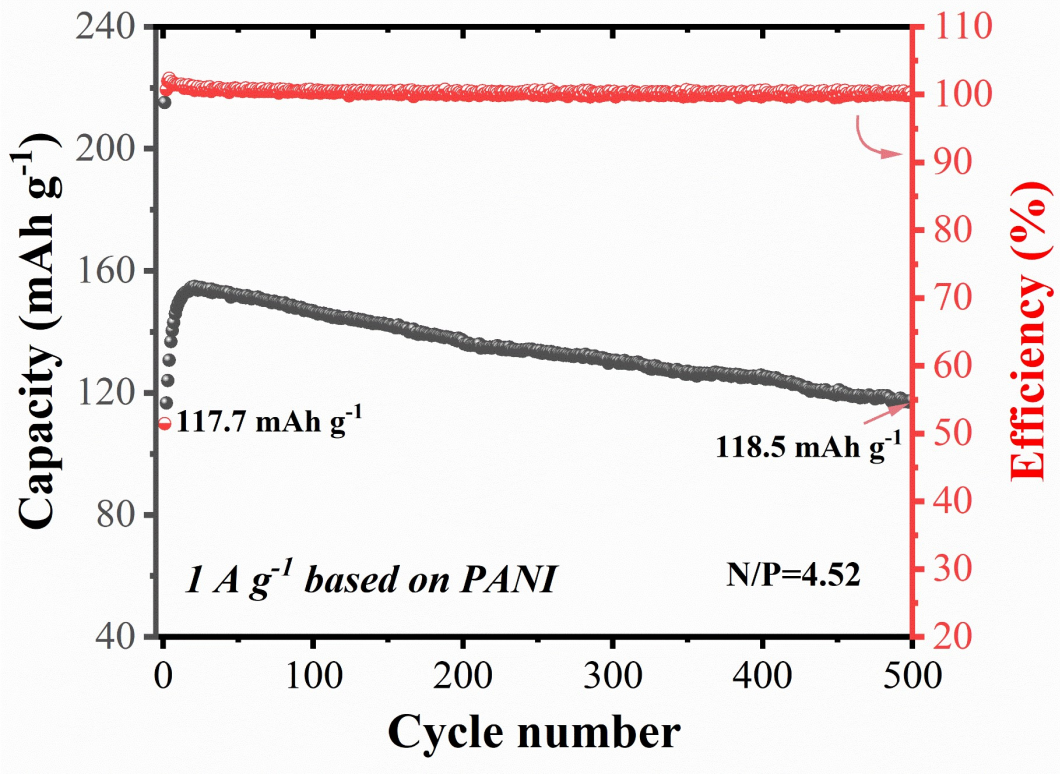

Figure S15. Long cycle performance of Cu@G@Zn//PANI battery at N/P=4.52.

Table S1. Summary of reported strategies for optimizing Zn anodes with graphene and its derivatives.

Materials	**Preparation methods**	**Material**	**Mechanism**	**Ref.**
G@SS	Doctor blading	graphene	Inducing Zn(002) orientatioanl deposition	*Science* 2019, 366, 645
N-VG@CC	Plasma enhanced chemical vapor deposition	N/O co-doped vertical graphene	Providing zincophility sites	Adv. Funct. Mater. 2021, 31, 2103922
Gr-modified Cu	Chemical vapor deposition	graphene	Inducing Zn(002) orientatioanl deposition	ACS Appl. Mater. Interfaces 2019, 11, 44077
$Ti_3C_2T_x$ MXene-reduced graphene oxide aerogels	freeze-dried	MXene and rGO	Inducing Zn uniform deposition	Adv. Energy Mater. 2023, 13, 2301557.
3DG@ZN	3D printing	Functionalized GO	Improving conductivity and regulating Zn^{2+} distribution	Energy Storage Mater. 2023, 54, 75
3D-RFGC@Zn	Thermal-chemical vapor deposition	3D N-doped Gr nanofibers/clusters and vertical Gr arrays	Providing zincophility sites	Nat. Commun. 2023, 14, 4205
EBP-NG/Zn	Langmuir-Blodgett method	N-doped graphene and black phosphorus nanosheets	Inducing Zn(002) orientational deposition	Energy Storage Mater. 2023, 56, 468
arranged GO sheets@Zn	Freeze-drying and thermal mild reduction	GO derivative	Providing zincophility sites	Adv. Mater. 2023, 35, 2205206
NOC@Zn	Plasma enhanced chemical vapor deposition	N/O co-doped mosaic nanocrystalline graphene structure	Inducing Zn(002) orientatioanl deposition	Adv. Sci. 2023, 10, 2206077
CNG/Zn		Cellulose nanowhisker and graphene	Inducing Zn(002) orientational deposition	Energy Environ. Sci. 2021, 14, 3120
NGO@Z	Langmuir-	N-doped GO	Providing	Adv. Mater. 2021, 33,

n	Blodgett method		zincophility Sites	2101649
EBP-NG	Step-by-step coating strategy	Exfoliated black phosphorus N-doped graphene	Providing zincophility sites and inducing Zn(002) orientational Deposition	Energy Storage Mater. 2023, 56, 468
ZGL@Zn	Doctor blading	ZIF-8, GO and PVDF	/	Energy Storage Mater. 2022, 47, 602

Table S2. Comparison of performances of Zn//Cu cells with those of the latest reported literatures in terms of three parameters: ACE, current density × per-cycle capacity, cumulative plated capacity (CPC).

Sample	mA cm^{-2} × mA h cm^{-2}	Cycle number	ACE (%)	CPC (mA h cm^{-2})	Ref
Cu@G	**80**	**6900**	**99.977**	**13,860**	**This work**
Cu@G	**100**	**1500**	**99.908**	**3000**	**This work**
LLP@Treated	5	1200	99.37	1200	ACS Energy Lett. 2023, 8, 8, 3297–3306.
ZIF	25	300	99.4	1500	Adv. Sci.2020,7, 2002173.
$Zn_3(PO_4)_2/ZnF_2$	8	90	99.37	180	Energy Environ. Sci., 2021,14, 3609-3620.
Nafion-Zn-X	0.25	130	97	75	Angew.Chem.Int.Ed.2020,59,16594–16601.
ZnS	2	200	99.2	200	Adv.Mater.2020, 32, 2003021.
Mxene	0.25	160	98.1	80	Energy Stor. Mater. 62 (2023) 102921.
β-PVDF	0.0648	200	96.9	36	Chem. Eng. J. 411 (2021) 128584.
60alucone	0.25	80	98.6	40	J. Mater. Chem. A, 2020,8, 22100-22110.
ZrO_2	5	220	95.5	220	Adv. Funct. Mater.2020, 30, 1908528.
ZnO-3D	1	300	99.55	150	Energy Environ. Sci., 2020,13, 503-510.
TiO_2/PVDF	1.56645	1000	99.4	88.5	Adv. Funct. Mater.2021, 31, 2001867.
Sc_2O_3	0.6328	260	99.85	145.6	J. Energy Chem. 55 (2021) 549–556.
SPEEK-Zn	1	600	99.47	600	Energy Stor. Mater. 49 (2022)

					380–389.
502-glue	2	200	99.74	200	Energy Stor. Mater. 36 (2021) 132–138.
USL	1	600	99.34	600	Nano Energy 103 (2022) 107751.
PDMS/TiO_{2-x}	10	700	99.6	700	Adv.Mater.2022, 34, 2105133.
ACG	0.5	2000	99.8	1000	J. Am. Chem. Soc. 2022, 144, 25, 11168–11177.
PA	2	800	99.9	800	Energy Environ. Sci., 2022,15, 1872-1881.
CAZ	0.25	750	99.8	375	Small 2022, 18, 2203327.
PI	8	1000	99.5	2000	Adv.Mater.2021, 33, 2007497.
Fluorinated interphase	0.25	1000	99.9	500	Nat. Nanotechnol. 16(8) (2021) 902-910.
ITO	2	1100	99.9	1100	Angew. Chem.Int. Ed.2023,62, e2023084.
3D-NC	2	130	97.6	130	J. Mater. Chem. A, 2022,10, 17440-17451.
ZnF_2	5	1000	99.5	1000	Adv.Mater.2021, 33, 2007388.
Cu@AOF	10	6000	99.9	6000	Adv. Energy Mater. 2023, 13, 2204388.
Cu@AOF	200	450	99.82	4500	Adv. Energy Mater. 2023, 13, 2204388.
C/Cu	0.5	300	99.6	150	Nano Lett. 2021, 21, 3, 1446–1453.
SIR	1	1000	99.7	1000	Angew. Chem.Int. Ed.2022,61,e2021 14789.
ex-ZrP	18	200	99.5	600	Energy Environ. Sci., 2022,15, 1682-1693.

Zn(101)	150	160	99.3	1600	Adv. Mater. (2023) 2305988.
Etched Zn	10	4500	99.92	4500	Energy Environ. Sci., (2023).
NGO	5	300	99.5	300	Adv.Mater.2021, 33, 2101649.
Carbon dots	0.25	1000	99.3	500	Adv. Energy Mater. 12(26) (2022) 2200665.
EBP-NG	1	1140	99.66	570	Energy Stor. Mater. 56 (2023) 468–477.
CNG	0.25	300	99.4	150	Energy Environ. Sci., 2021,14, 3120-3129.
FLG	1	100	98	100	J. Alloys Compd. 891 (2021) 161886.
N-C	4	120	98.76	240	Dalton Trans., 2020,49, 17629-17634.
NOC	10	800	99.5	800	Adv. Sci.2023,10, 2206077.
Graphene	64	10000	99.9	16,000	Science 366, 645–648 (2019).
Graphene	128	2250	99.7	7200	Science 366, 645–648 (2019).

Reference:

[1] a)G. Kresse, J. Furthmüller, *Physical Review B* **1996**, 54, 11169; b)G. Kresse, D. Joubert, *Physical Review B* **1999**, 59, 1758.

[2] J. P. Perdew, K. Burke, M. Ernzerhof, *Physical Review Letters* **1996**, 77, 3865.

[3] S. Grimme, J. Antony, S. Ehrlich, H. Krieg, *The Journal of Chemical Physics* **2010**, 132, 154104.